Photoproduction of Single Top at LHC

Vincent Lemaitre, Jérôme de Favereau, Sverine Ovyn, Krzysztof Piotrzkowski

Center for Particle Physics and Phenomenology (CP3)
Université catholique de Louvain
Chemin du cyclotron 2, 1348 Louvain-la-Neuve, Belgium

DOI: http://dx.doi.org/10.3204/DESY-PROC-2009-03/Lemaitre

High-energy photon-proton interactions at the LHC offer interesting possibilities for the study of the electroweak sector up to TeV scales and searches for processes beyond the Standard Model. In particular, after 10 fb-1, the analysis of W associated single top photoproduction events can provide a sensitivity to $|V_{tb}|$ comparable to the one obtained using the standard single top production in pp collisions. Study of photoproduction at the LHC provides also an ideal framework for observing anomalous productions of single top induced by Flavour-Changing Neutral Currents.

1 Introduction

A significant fraction of *pp* collisions at the LHC will involve (quasi-real) photon interactions occurring at energies well beyond the electroweak energy scale [1]. The LHC can therefore be considered to some extend as a high-energy photon-proton collider. In a recent paper [2], several studies of high energy photon interactions at the LHC were reported. In particular, it is shown that a large variety of $pp(\gamma g/q \to X)pY$ processes have sizable cross section and could therefore be studied during the very low and low luminosity phases of LHC. Interestingly, the SM inclusive photoproduction cross section of top quark reaches 2.5 pb and the fraction of single top to top quark pair cross sections is close to one. This large ratio offers an interesting framework for the studies of top properties which can only be addressed from single top production mechanism such as the CKM $|V_{tb}|$ matrix element. Probing possible anomalous photoproduction of single top via flavour-changing neutral currents (FCNC) is also particularly relevant at the LHC since the expected cross section calculated with the present limits on the anomalous couplings $k_{tq\gamma}$ is close to 10 pb.

2 Tagging photoproduction

Tagging is essential for the extraction of high energy photon-induced interactions from the large parton-parton interactions. Photon-induced interactions are characterised by a large pseudo-rapidity region completely devoid of any hadronic activity. This region is usually called *large rapidity gap* (LRG).

2.1 Very low luminosity phase ($< 10^{33}$ cm^{-2}s^{-1})

The number of extra interactions per beam crossing (*pile-up*) is negligible at very low luminosity. Thanks to the colour flow in *pp* interactions between the proton remnant and the hard hadronic final states, a simple way to suppress generic *pp* interactions is to require LRGs by looking at the energy measured in the forward detector containing the minimum forward activity (between $3 < |\eta| < 5$), denoted as E^{FCal}. For a maximal allowed energy of 50 GeV, a typical reduction factor of 10^{-3} and 10^{-2} for a parton-parton $t\bar{t}$ and Wj production is expected, respectively. A total integrated luminosity of 1 fb^{-1} for such no *pile-up* condition seems to be a realistic assumption. The rejection can be further improved by using an exclusivity condition requiring no additional tracks (*i.e.* excluding isolated leptons and jet cones) with $p_T > 0.5$ GeV/c and $1 < \eta < 2.5$ in the hemisphere where the rapidity gap is present. It should be pointed out that this condition can also be used during the higher luminosity phases if proper vertex determination is possible. The efficiency of rapidity gap and exclusivity conditions for signal processes drops roughly by a factor of two while the reduction factors for parton-parton reactions are better than 10^{-3}.

2.2 Low luminosity phase

When event *pile-up* increase to much, the LRG technique cannot be used, and the exclusivity condition alone cannot reduce partonic backgrounds to a level that allows proper signal extraction. Therefore, in addition to the exclusivity condition, the use of *very forward detectors* (VFD) to detect the escaping proton is mandatory in order to retain *pp* background low. However, VFDs cannot provide a total rejection of the partonic processes because of the presence of single diffractive events in the *pile-up*. Hence, the overall event mimics well a photoproduction event. The probability of such accidental coincidences provides directly the rejection power of VFDs. For instance, the case for which VFD stations would be put at 220 m and 420 m from the interaction point has been computed and provides rejection factors of 11 and 5.6 for a luminosity of 10^{33} cm^{-2} s^{-1} and 2×10^{33} cm^{-2} s^{-1}, respectively.

3 Cross section and event simulation

All cross sections and event samples used in this analysis have been obtained using the adapted MadGraph/MadEvent [4, 5] and CalcHEP [6] programs (except for some induced proton-proton induced backgrounds where Alpgen was used). Cross sections are therefore calculated at Leading order and do not include any survival probability factor. In order to take into account the effect of jet algorithms and the efficiency of event selection under realistic experimental conditions, the generated events were passed: (1) to PYTHIA 6.227 [7] and (2) a fast simulation of a typical LHC multi-purpose detector.

The detector response simulation is performed using Delphes assuming geometrical acceptance of sub-detectors and their finite energy resolutions. The default card provided to simulate the CMS detector has been used and the jets are reconstructed using the MidPointCone algorithm with a cone radius of $\Delta R = 0.7$. A proper simulation of the proton propagation in the LHC beamline performed using HECTOR [11], shows that using detectors stations at 220 m and 420 m from the IP, one selects events for which the proton has lost between 20 GeV and 800 GeV. Magnetic field was also taken into account when evaluating the forward energy deposits. The transverse missing energy is calculated from the calorimetric towers. When heavy

flavour tagging is required, a tagging efficiency of 40% , 10%, and 1% has been applied for b-, c-, and light- jets respectively.

Another possible background source not simulated in this analysis is the Inelastic photoproduction, in which the proton having emitted a photon does not survive the interaction. It should be stressed that Inelastic photoproduction would actually increase the cross section of both signal and photon-induced backgrounds.

4 W associated single top photoproduction

Photoproduction of single top is dominated by t-channel amplitudes when the top quark is produced in association with a W boson (Fig. 1). These amplitudes are all proportional to the CKM $|V_{tb}|$ matrix element.

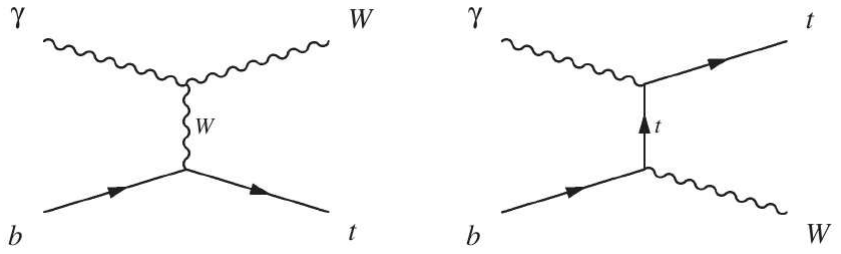

Figure 1: Diagrams for the dominant contribution to the SM production of single top quark.

The $pp(\gamma q \to Wt)pY$ process results in a final state of two on-shell W bosons and a b quark. The studied topologies are ℓbjj for the semi-leptonic decay of the two W bosons and $\ell\ell b$ for the di-leptonic decay, where $\ell = e,\ \mu$ or τ. The cross sections times branching ratios of these final states are 440 fb and 104 fb respectively. The dominant irreducible background of both channels is expected to stem from the $t\bar{t}$ production, where a jet misses the acceptance region. Other backgrounds are $Wb\bar{b}q'$, $Wjjj$ and WWq' processes produced either from photon-proton interactions, or from proton-proton interactions. Their cross sections including the branching ratio into the desired topology are summarised in Tab. 1.

4.1 Signal selection

For the semi-leptonic final state, the following "acceptance cuts" are applied: one isolated lepton with $p_T^\ell > 20$ GeV/c; exactly 3 jets with $p_T^j > 30$ GeV/c. Lepton isolation requires that there is no other charged particles with $p_T > 2$ GeV/c within a cone of $\Delta R < 0.5$ around the lepton. Partonic backgrounds are reduced by requiring the E^{FCal} condition with a cut value of 30 GeV as well as the exclusivity condition (γp cuts).Moreover, exactly one of the three jets must be identified as a b-jet (b-tagged). In addition, the invariant mass of the two non b-tagged jets must satisfy $|m_W - m_{jj}| < 20$ GeV/c^2 and the scalar sum of the visible particles must be smaller than 230 GeV/c ("Final cuts").

After this selection, the final cross section times branching ratio for the signal is reduced to 5.6 fb, against 5.2 fb for the backgrounds, 52 % of which comes from partonic processes. The

Process		$\sigma\times$ Br [fb]	sample size
$\gamma p \rightarrow$	$t\bar{t}(2\ell)$	159.1	200 k
	$t\bar{t}(1\ell)$	671.8	179 k
	$WWq'(2\ell)$	62.5	70 k
	$Wjjj$	2793.0	50 k
	$Wb\bar{b}q'$	55.2	10 k
$pp \rightarrow$	$t\bar{t}(2\ell)$	77.7×10^3	130 k
	$t\bar{t}(1\ell)$	328×10^3	390 k
	$W2j$	2.4×10^6	830 k
	$W3j$	6.9×10^5	264 k
	$W4j$	1.7×10^5	105 k
	$Wb\bar{b}j$	2.7×10^5	120 k
	tj	6.7×10^3	100 k
	$WWj(2\ell)$	5.2×10^3	100 k

Table 1: Background processes used in the semi-leptonic and di-leptonic channels. Cross-sections include generation cuts of $p_T > 1$ GeV/c for q' and $p_T > 10$ GeV/c for jets. Branching ratios quoted in parenthesis are also taken into account. The $W2j$, $W3j$ and $W4j$ have been generated using Alpgen with a minimal p_T^{cut} on the jets of 20 GeV/c. Branching ratio of the W boson into leptons (e, μ or τ) is taken into account.

$t\bar{t} \rightarrow \ell\ell bb$ topology is also taken into account in the backgrounds. Details are given in Tab. 2. The visible cross sections obtained using the expected rejection of 11 for the low luminosity phase $\mathcal{L} = 10^{33}$ cm^{-2} s^{-1} are also shown. In this case, the large number of partonic events is mainly due to $pp \rightarrow W$jets events.

σ [fb]		signal	γp backgrounds	pp backgrounds
Production		440.6	3.6×10^3	74×10^6
Acceptance cuts		39.1	152.5	126×10^3
γp cuts	Very low $\mathcal{L}$	27.4	90.7	127.1
	Low $\mathcal{L}$	27.4	85.5	873.7
Final cuts	Very low $\mathcal{L}$	5.6	2.4	2.8
	Low $\mathcal{L}$	5.6	2.2	18.6

Table 2: List and effect on the visible cross-section of all applied cuts on the $\gamma p \rightarrow Wt \rightarrow \ell\nu jjb$ events and their relevant photon-induced and proton-induced backgrounds. Very low luminosity refer to $\mathcal{L} < 10^{33}$ cm^{-2} s^{-1} and Low luminosity refers to $\mathcal{L} = 10^{33}$ cm^{-2} s^{-1}.

The procedure to select the di-leptonic topology is simpler: it requires two isolated lepton with $p_T > 20$ GeV/c; one b-tagged jet with $p_T^b > 30$ GeV/c and no additional jets with $p_T^j > 30$ GeV/c. The same rapidity gap and exclusivity condition as in the semi-leptonic topology are applied. Signal cross section times branching ration for this topology is 5.9 fb after cuts, for a background cross section of 3.1 fb with less than 40 % of partonic contribution (32%). Details are in Tab. 3. During the phase of low luminosity, using forward proton taggers, event if the number of partonic event is less important than for the semi-leptonic case, the signal to

background ratio decreases from 1.6 to 0.4.

σ [fb]		signal	$t\bar{t}$		WWq'	
			γp	pp	γp	pp
Production		104.3	159.1	77×10^3	62.5	5×10^3
Acceptance cuts		15.6	10.5	3.4×10^3	4.2	486
γp cuts	Very low $\mathcal{L}$	14.3	4.9	1.8	4.0	0.6
	Low $\mathcal{L}$	12.8	4.8	24.0	3.4	4.2
Final cuts	Very low $\mathcal{L}$	5.9	2.0	0.8	0.1	0.2
	Low $\mathcal{L}$	5.0	1.9	9.1	0.1	1.1

Table 3: List and effect on the visible cross-section of all applied cuts on the $\gamma p \to Wt \to \ell\nu\ell\nu b$ events and their relevant photon-induced and proton-induced backgrounds. Very low luminosity refer to $\mathcal{L} < 10^{33}$ cm^{-2} s^{-1} and Low luminosity refers to $\mathcal{L} = 10^{33}$ cm^{-2} s^{-1}.

4.2 Systematic errors

When no estimate on the theoretical uncertainties is found in the literature for photon-proton cross sections, a conservative attitude was adopted in taking the same uncertainty as for the corresponding partonic process. Partonic cross sections after cuts are considered to be known to the 2 % level as the cross section without application of the E^{FCal} and exclusivity conditions can be measured directly and the error on the effect of these cuts is computed separately. The most relevant detector systematics are expected to be the uncertainties on the Jet Energy Scale (JES), the number of reconstructed tracks in order to apply the exclusivity condition and the energy measurement in the forward calorimeter. The uncertainty due to JES is expected to be 5% for jets with $p_T < 30$ GeV/c, 3% for jets with $p_T > 50$ GeV/c and a linear interpolation between these two boundaries. The systematic uncertainty due to the exclusivity condition is estimated by moving the track reconstruction efficiency, fixed to 90 % by default, to 85% and 95%. Finally, the cut on the energy in the forward calorimeter of the gap side has been moved by 10 % upwards and downwards in order to have an idea of the E^{FCal} condition uncertainty. The b-tagging uncertainty is taken as $\pm$5%, while the error on mis-tagging is assumed to be 10%. The uncertainty due to luminosity is expected to be 5%.

All systematic errors between the different samples have been assumed to be 100% correlated and are therefore applied simultaneously on all samples except for the theoretical errors. The different error sources are supposed to be uncorrelated and are therefore added quadratically. For both topologies, the error is dominated by the rapidity gap and exclusivity cuts uncertainties on the pp induced backgrounds.

4.3 Results

A simple propagation of errors shows that the relative uncertainty on the measured cross section is given by the following formula :

$$\frac{\Delta\sigma_{obs}}{\sigma_{obs}} = \frac{\Delta\varepsilon}{\varepsilon} \oplus \frac{\Delta L}{L} \oplus \left[\frac{B}{S}\right] \frac{\Delta B}{B} \oplus \left[\frac{B}{S} + 1\right] \frac{\Delta N}{N},$$

where $\Delta\varepsilon$, ΔL and ΔB are the systematic errors estimates on the signal selection efficiency, the luminosity and the background cross section respectively and ΔN is the statistical error on the observed number of events. The uncertainties obtained for the di-leptonic and the semi-leptonic topologies after an integrated luminosity of 10 fb^{-1} are summarised in Tab. 4. Comparing these errors on the cross section to the expected one from parton-parton interactions, 10 % in the *t-channel*, 31 % in the *s-channel*, 25.8 % for the di-leptonic and 22.6 % for the semi-leptonic topologies in the *tW-channel* [8] using the same integrated luminosity, we can conclude that photoproduction is at least competitive with partonic-based studies and that the combination of both studies could lead to significant improvement of the error.

Error	Di-leptonic [%]		Semi-leptonic [%]	
$\mathcal{L}$	Very low	Low	Very low	Low
$\frac{\Delta\varepsilon}{\varepsilon}$	5.0	5.02	9.2	9.1
$\frac{\Delta L}{L}$	5.0	5.0	5.0	5.0
$\left[\frac{B}{S}\right]\frac{\Delta B}{B}$	10.3	25.9	19.5	68.1
$\left[\frac{B}{S}+1\right]\frac{\Delta N}{N}$	16.4	26.2	9.7	29.1
total	20.6	37.6	27.9	74.8

Table 4: Contributions to the total cross-section measurement error.

Taking into account a 5% uncertainty on the theoretical total single top cross section,the expected error on the measurement of $|V_{tb}|$ is 14.3% for the semi-leptonic channel and 10.7% for the di-leptonic one after 10 fb^{-1} of integrated luminosity. Assuming the same integrated luminosity during the low luminosity phase of the LHC ($\mathcal{L} = 10^{33}$ cm^{-2} s^{-1}) the two obtained values are respectively 37.5% and 19.0%.

5 Anomalous single top photoproduction

FCNC appear in many extensions of the Standard Model, such as two Higgs-doublet models or R-Parity violating supersymmetry. Such a FCNC transition can occur in the process of single top photoproduction via anomalous couplings, as shown on Fig. 2. The effective Lagrangian for these anomalous coupling can be written as [9]:

$$\mathcal{L} = iee_t\bar{t}\ \frac{\sigma_{\mu\nu}q^\nu}{\Lambda}\ k_{tu\gamma}uA^\mu + iee_t\bar{t}\ \frac{\sigma_{\mu\nu}q^\nu}{\Lambda}\ k_{tc\gamma}cA^\mu + h.c.,$$

where $\sigma^{\mu\nu}$ is defined as $(\gamma^\mu\gamma^\nu - \gamma^\nu\gamma^\mu)/2$, q^ν being the photon 4-vector and Λ an arbitrary scale, conventionally taken as the top mass. The anomalous couplings $k_{tu\gamma}$ and $k_{tc\gamma}$ are real and positive such that the cross section takes the form

$$\sigma_{pp\to t} = \alpha_u\ k^2_{tu\gamma} + \alpha_c\ k^2_{tc\gamma}.$$

The computed α parameters obtained using CalcHEP are $\alpha_u = 368$ pb and $\alpha_c = 122$ pb. The present best upper limit on $k_{tu\gamma}$ is around 0.14, depending on the top mass [10] while the anomalous coupling $k_{tc\gamma}$ has not been probed yet.

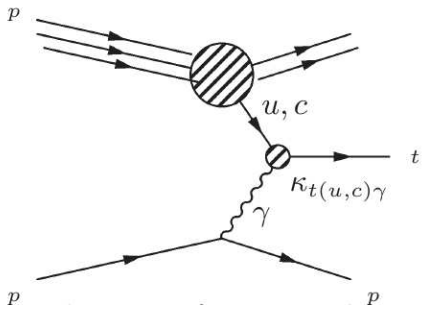

Figure 2: Main diagram for FCNC production of single top.

The studied final state consists in one hard lepton and missing transverse energy issued from the W boson coming from the top quark decay, which produced as well a b quark. The dominant background processes for this final state come from events with one W boson and one jet mis-tagged as a b-jet. We assumed no contribution of genuine b-jets since its cross section is three orders of magnitude lower than the cross section of the Wc topology. Backgrounds cross sections and sample sizes are given in Tab. 5.

Process	σ [fb]	sample size
$\gamma p \to Wj$	41.6×10^3	100 k
Wc	11.5×10^3	100 k
$pp \to Wj$	77.3×10^6	100 k
Wc	8.8×10^6	100 k
Diffractive W	1.3×10^6	100 k

Table 5: Background processes used for the analysis of the anomalous top photoproduction. Cross-sections include the branching ratio of the W boson to electron or muon and generation cuts of $p_T > 10$ GeV/c for leptons and $p_T > 20$ GeV/c for jets (j=u,d,s,and g).

5.1 Signal selection

Preselection cuts require the presence of exactly one jet with $p_T > 45$ GeV/c, one isolated lepton with $p_T > 20$ GeV/c, and a transverse missing energy above 15 GeV. These cuts designed to reject pp interactions in the scheme of zero pile-up conditions are applied with a maximum allowed energy in the forward hemisphere of 20 GeV. An event is selected if the only allowed jet is tagged as a b-jet and a top candidate is also reconstructed from the W-boson and the "b-jet" with a mass between 140 GeV and 210 GeV.

In order to extend this study in presence of event *pile-up*, the use of the E^{FCal} selection cut is replaced by the tagging of the escaping proton by VFDs as described in section 2. As stated before, the reduction of the partonic background is less effective than the one obtained in zero *pile-up* condition. However, another advantage of the VFD is that, considering a well designed reconstruction algorithm, the energy loss of the proton that hits the VFD can be determined and

used to improve the selection of photoproduction processes. An additional cut is therefore used that reconstructs the top quark longitudinal momentum both from the central event and from the proton energy loss. The difference between these two values allows to distinguish between photoproduction events for which they are close, and partonic events for which the distance between them is distributed randomly.

5.2 Systematic errors

The same systematic uncertainties as in the case of the SM single top study have been estimated. Once again, the rapidity gap and exclusivity condition account for the most important part of it. In the case of low luminosities (corresponding here to $\mathcal{L} = 2 \times 10^{33}$ cm^{-2} s^{-1}) for which the VFDs where used, no systematic error is assumed on this tagging. The detail of all errors for both scenario's are given on Tab. 6. Signal systematics stay unaffected by the scenario change, as the error due to the LRG requirement is negligible. The uncertainty on the diffractive cross section has been set to 50%.

Error	signal (%)	Background (%)				
		$\gamma p \to Wj$	$\gamma p \to Wc$	$pp \to Wj$	$pp \to Wc$	Diffr. W
JES	1.6	2.0	3.0	4.0	3.1	-
Exclusivity	1.0	1.0	1.0	10.0	10.0	-
LRG	0.0	0.0	0.0	20.0	20.0	-
Luminosity	5.0	5.0	5.0	5.0	5.0	-
b-tagging	5.0	10.0	5.0	10.0	5.0	-
Theoretical	5.0	5.0	5.0	2.0	2.0	50
total	8.9			18.6		

Table 6: Systematic errors on signal and backgrounds at very low luminosity.

5.3 Results

Using the LRG requirement for an integrated luminosity of 1 fb^{-1}, one gets the following number of events (for $k_{tu\gamma} = 0.15$, $k_{tc\gamma} = 0$) : 129 signal events, 13.2 background events from photoproduction, 10 events from pp induced backgrounds and 12 diffractive events. The corresponding expected 95% C.L. limit for the anomalous couplings are: $k_{tu\gamma} < 0.024$, $k_{tc\gamma} < 0.039$. These limits can be further improved by a factor two when collecting a few then of inverse femptobarns at low luminosity regime.

6 Conclusions and prospects

Top quark photoproduction cross section is large and, in particular, the Wt associated production can be studied with a much better signal to noise ratio as the corresponding process induced by generic pp collisions. This process could permits, for instance, to extract $|V_{tb}|$ with a similar accuracy but with an error which is dominated by the statistical error.

Photoproduction at LHC can probe electroweak and BSM theories at c.m.s energy up to 2 TeV with sizable cross sections. For instance, anomalous single top photoproduction has a similar sensitivity to anomalous FCNC couplings than analyses based on rare top decays.

However, the studies presented in this paper will be refined when full detector simulation will be used, providing a better estimate of the systematic errors. Also, studying the influence of diffractive backgrounds on $|V_{tb}|$ is an important part of the work to be done, as well as the evaluation of the contribution of inelastic photon emissions to both signal and backgrounds.

References

[1] K. Piotrzkowski, Phys. Rev. D**63**, (2001) 071502.

[2] J. de Favereau et al, to be published

[3] The CMS Collaboration, J. Phys. G**34** (2007) 1237-1240.

[4] J. Alwall et al., JHEP**09**, (2007) 028.

[5] T. Stelzer and W.F. Long, Phys.Commun.**81**, (1994) 357-371.

[6] A. Pukhov, Nucl. Inst. Meth A**502**, (2003) 596-598.

[7] T. Sjöstrand et al., Comput. Phys. Commun. **135**, (2001) 238.

[8] The CMS Collaboration, J. Phys. G**34** (2007) 1227-1237.

[9] T. Han and J.L. Hewett, Phys. Rev. D**60**, (1999) 074015.

[10] S. Chekanov et al., Phys. Lett. B**559**, (2003) 153-170.

[11] J. de Favereau de Jeneret, X. Rouby, K. Piotrzkowski, JINST 2 P09005, arXiv:0707.1198v1 [physics.acc-ph] (CP3-07-13).